# Crystal supramolecular motifs: two-dimensional grids of terpy embraces in $[ML_2]^z$ complexes (L = terpy or aromatic $N_3$-tridentate ligand)

**Marcia L. Scudder, Harold A. Goodwin and Ian G. Dance***

*School of Chemistry, University of New South Wales, Sydney 2052, Australia.*
*E-mail: I.Dance@unsw.edu.au*

***Received* (*in Montpellier, France*) *19th January 1999, Accepted 29th March 1999***

By analysis of crystal packing we have identified a crystal supramolecular motif that is a two-dimensional net of terpy embraces formed by metal complexes $[M(terpy)_2]^{2+}$ (terpy = 2,2′ : 6′,2″-terpyridyl) and similar meridional $[M(N_3\text{-tridentate})_2]$ complexes. The terpy embrace involves two complexes attracted by one offset-face-to-face (**off**) and two edge-to-face (**ef**) interactions by the outer pyridyl rings of the ligand. In many crystals containing small monoanions there is a two-dimensional net of these embraces, in which each complex forms eight **ef** and four **off** interactions with its neighbours. The principal axes of the complexes are normal to the layer, which is exactly or approximately planar, and can occur with high (tetragonal) or low crystal symmetry. Grooves that occur on the layer surfaces, formed between parallel central pyridyl rings of the ligands, run in orthogonal directions on the two surfaces of each layer. Anions and solvent molecules in the crystals are usually disordered, in or near the grooves. The net attractive energy of the terpy embrace for a pair of $[M(terpy)_2]^{2+}$ is calculated to be *ca.* 15 kJ mol$^{-1}$: in the two-dimensional net the attractive cation···cation energy per cation is *ca.* 29 kJ mol$^{-1}$. Inclusion of the anions associated with one layer increases the attractive energy per $[M(terpy)_2]^{2+}$ to the order of 130 kJ mol$^{-1}$. A variety of ligands, which are minor or major modifications of terpy, also form this supramolecular motif. Hydrogen bonding involving NH functions of these ligands, solvent, and/or anions, does not in general disrupt the motif. In one instance where the $[M(N_3\text{-tridentate})_2]$ complex is uncharged there is mutual interpenetration of contiguous layers. These infinite two-dimensional nets of octahedral metal complex sites formed as crystal supramolecules are analogous to the two-dimensional gridlike supermolecules formed by extended oligo-chelating ligands. Opportunities for crystal engineering are discussed.

Phenyl groups on the surfaces of molecules are the sites of a considerable amount of intermolecular attractive energy, through the well-known edge-to-face (**ef**) and offset-face-to-face (**off**) phenyl–phenyl interactions, which can contribute up to 10 kJ mol$^{-1}$.[1] In recent papers[2–10] we have described a number of supramolecular motifs in which molecules with arrays of phenyl groups come together to form a set of **ef** and/or **off** local interactions acting in concert. These supramolecular motifs are named multiple phenyl embraces, and they are widely evident in the molecular packing in the crystal structures of these compounds. For example, about 30% of the known crystals containing $Ph_4P^+$ demonstrate the sixfold phenyl embrace (6PE) with six concerted **ef** interactions involving six phenyl rings in the interaction zone, with a total attractive energy of *ca.* 45 kJ mol$^{-1}$. It is significant that the net cation···cation interactions in these motifs and crystals are attractive.

While the 6PE is the most frequently occurring concerted phenyl embrace, there are others, incorporating varying numbers of aromatic rings. There are two common variants of the 4PE. One, the O4PE (orthogonal4PE[3]), is similar to the 6PE in that there is a cycle of edge-to-face interactions between the four phenyl rings taking part in the embrace. The P4PE (parallel4PE[3]) is different, in that it is a composite of **ef** and **off** interactions.

† Supplementary material available: a more detailed description of the crystal structures under consideration. For direct electronic access see http://www.rsc.org/suppdata/nj/1999/695/, otherwise available from BLDSC (No. SUP 57552, 14 pp.) or the RSC Library. See Instructions for Authors, 1999, Issue 1 (http://www.rsc.org/njc).

Other aromatic and heteroaromatic components of molecules can also take part in similar motifs. For example, we have found[11] that there is a crystal supramolecular motif common to many of the structures of metal complexes of the type $[M(bipy)_3]^{0/2+}$. The molecules are aligned in the crystal structure so that their threefold (or pseudo threefold) axis is parallel to a chain, along which each cation takes part in two sixfold aryl embraces (6AE), which are analogous to the 6PE because there is a concerted cycle of six edge-to-face interactions involving pyridyl rings.

We now report that a majority of metal complexes of the type $[M(tridentate)_2]$, with meridional octahedral stereochemistry, form a crystal supramolecular motif in which the complexes are maintained in a two-dimensional net by local interactions that are analogous to the P4PE. Figgis *et al.*[12] first recognised a common crystal packing in compounds of the type $[Co(terpy)_2]^{2+}$, terpy = 2,2′:6′,2″-terpyridyl. We have extended the investigation to the larger number and wider range of complexes now known. We demonstrate the widespread occurrence, the general characteristics, and the limitations of this motif, and estimate the supramolecular energies that maintain it.

## Results

### The terpy embrace

We will first consider complexes of the ligand terpyridine, in which the central and outer rings will be distinguished as $R^c$ and $R^o$, respectively, and the $S_4$ axis of the complex is named the principal axis.

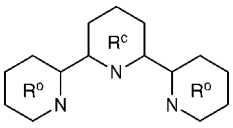


The two ligand planes in octahedral complexes $[M(terpy)_2]^z$ are exactly or almost orthogonal. When two such $[M(terpy)_2]^z$ molecules associate in crystals, they do so in a way that is analogous to the P4PE described above—the heterocyclic rings take part in two **ef** and one **off** interaction. Fig. 1 displays this "terpy embrace" between two $[M(terpy)_2]^{2+}$ molecules. All four of the ligands are involved, but only through their outer rings $R^o$. There is a pair of $R^o$ pyridyl rings in good **off** geometry in the centre of the embrace, and each of these rings also directs an edge towards the face of another $R^o$ pyridyl ring. Fig. 1(*a*) shows the perfect **ef** and **off** alignment, and Fig. 1(b), viewed normal to Fig. 1(a), shows the detail of the **off** overlap in which H atoms of one $R^o$ are adjacent to C atoms of the other. Both of these interactions allow the $H^{\delta+}\cdots C^{\delta-}$ intermolecular approaches that contribute attractive coulombic energy to this motif. The geometry for the **off** and **ef** interactions in the terpy embrace is similar to that of the P4PE shown in Fig. 1(c).

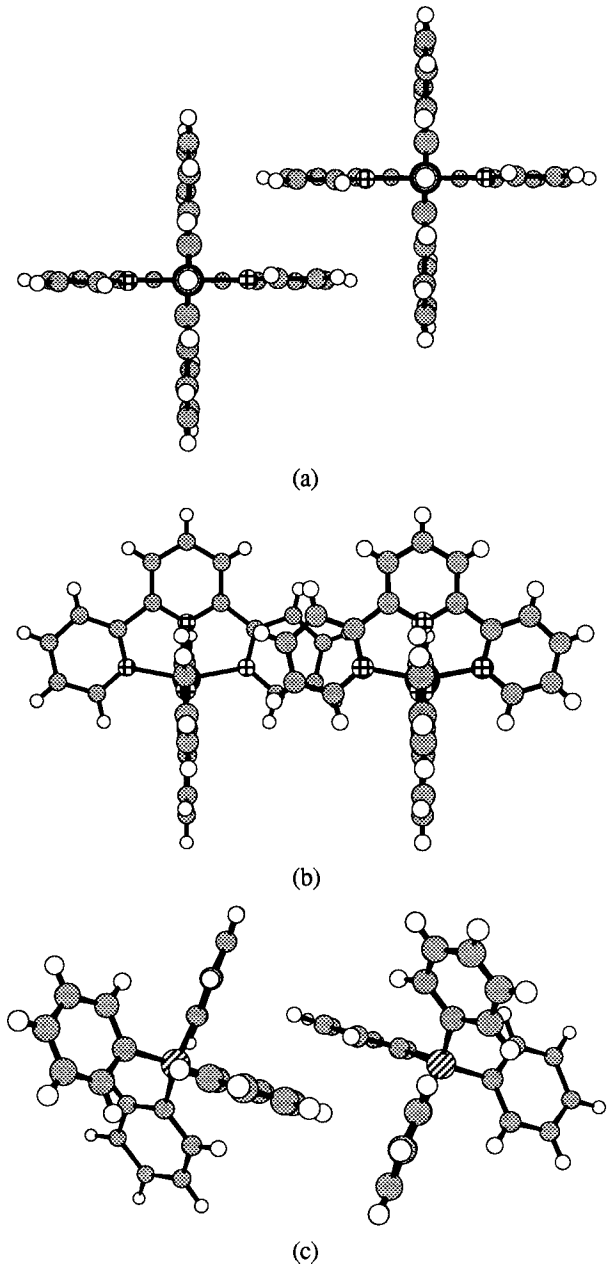


**Fig. 1** The fourfold terpy embrace of two $[Co(terpy)_2]^{2+}$ complexes: (a) is parallel to the principal axes of the two complexes; the ring···ring separation in the central **off** interaction is 3.6 Å and the H···C distance in each of the **ef** interactions is 2.9 Å. (b) is perpendicular to (a) and shows detail of the overlap of the **off** pair of rings, as well as a groove between the two parallel terpy ligands, which are acceptors in the **ef** interactions. The P4PE of two $Ph_4P^+$ molecules in (c) is comparable with the terpy embrace in (a).

### The two-dimensional net of terpy embraces

The terpy embrace is not restricted to a pair of molecules. Use of all of the $R^o$ rings generates a two-dimensional net of $[M(terpy)_2]$ molecules fully engaged in these terpy embraces, and these nets occur in crystal structures. Fig. 2(a) shows the concert of **ef** and **off** interactions in a cycle of four $[M(terpy)_2]$ molecules, while Fig. 2(b) shows a space-filling representation of part of an extended layer. The planes of the ligands are perpendicular to the layer, with ligands protruding from one side of the layer being parallel to each other, but orthogonal to those protruding from the other side. Each $[M(terpy)_2]$ molecule takes part in 12 interactions, eight **ef** and four **off**. Each $R^o$ ring participates in three interactions: one surface of each $R^o$ takes part in an **off** interaction while the other surface accepts an **ef** interaction, and the H atoms on the periphery of $R^o$ are the donor atoms of another **ef** interaction. In highly symmetrical crystal structures many of these interactions are equivalent. Fig. 2(c) shows how coplanarity of the metal centres in a layer allows the **ef** and **off** interactions of $R^o$ rings to be well developed.

### Grooves in the layers and the stacking of layers

The central rings of the terpy ligands are not involved in the **ef** and **off** local interactions that maintain the net, but protrude perpendicular to it, and form grooves [Fig 2(c)]. The anions in crystals are commonly associated with these grooves. The grooves are segmented, because the walls of the groove—the $R^c$ pyridyl rings—are not parallel to the centreline of the extended groove. The shapes of the grooves are shown clearly in Fig. 3, which presents part of the crystal structure of $[Mn(terpy)_2](I_3)_2$ [SIWFIN] in which the grooves are occupied by triiodide ions, with one $I_3^-$ fitting neatly into each groove segment. The grooves are approximately one pyridyl ring wide and less than one pyridyl ring deep [see Fig. 2(c)]. In the crystal structures described below there is variation in the shapes and sizes of the grooves.

The stacking of layers for $[M(terpy)_2]$ crystals is influenced by the C4′–H4′ bond of the central pyridyl ring: this is the bond on the $S_4$ axis of the complex. The C4′–H4′ bond is perpendicular to the layer, and furthest from the centre of the layer [see Fig. 2(c)]. The stacking of layers is such that this C4′–H4′ bond is directed into the central cavity between four $[M(terpy)_2]$ molecules in the contiguous layer. Fig. 4 shows the relationship between the locations and orientations of $[Co(terpy)_2]^{2+}$ molecules in two adjacent layers in the crystal structure of $[Co(terpy)_2]I_2 \cdot 2H_2O$ [CASXID].

There are two ways in which adjacent layers of terpy motifs are stacked in crystals. One is shown in Fig. 4 where the terpy ligand planes on either side of the layer interface are parallel to each other. The alternative is shown in Fig. 5 in which these ligand planes are at 45° to each other: alternating terpy layers in the stack are rotated by 45°. This occurs in the crystal structure of $[Cu(terpy)_2](PF_6)_2$ [BEJPUB] shown in Fig. 5.

### Generality and characteristics of the terpy layer motif

A survey of $[M(terpy)_2]^z$ crystal structures in the Cambridge Structural Database (October, 1998)[13,14] shows that the layer motif exists in almost all of them. Table 1 lists all of the

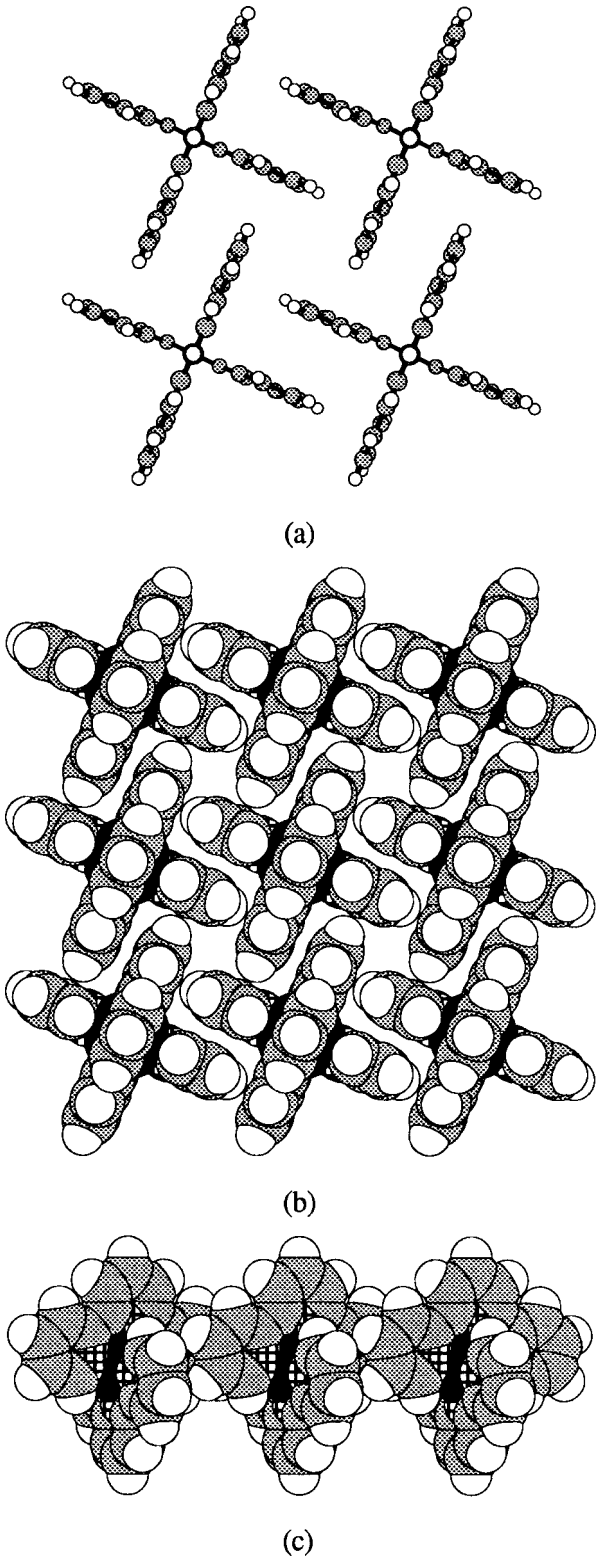


**Fig. 2** Representations of the two-dimensional net of terpy embraces in $[Co(terpy)_2]I_2 \cdot 2H_2O$ [CASXID]. (a) An array of four complexes showing the interlocking **ef** and **off** interactions. (b) Space-filling representation of a 3 × 3 array of molecules in the net. (c) A space-filling view parallel to the layer, showing detail of the **ef** interactions that involve terpy ligands on opposite sides of the layer. This also shows part of the grooves in the surfaces of the layer.

$[M(terpy)_2]^{2+}$ and $[M(terpy)_2]^{3+}$ crystalline compounds found in the CSD, plus two of our recently published structures. All except three of the $[M(terpy)_2]^{2+}$ compounds demonstrate the full two-dimensional terpy embrace motif, and the exceptions can be understood in terms of the disrupting supramolecular interactions (see below).

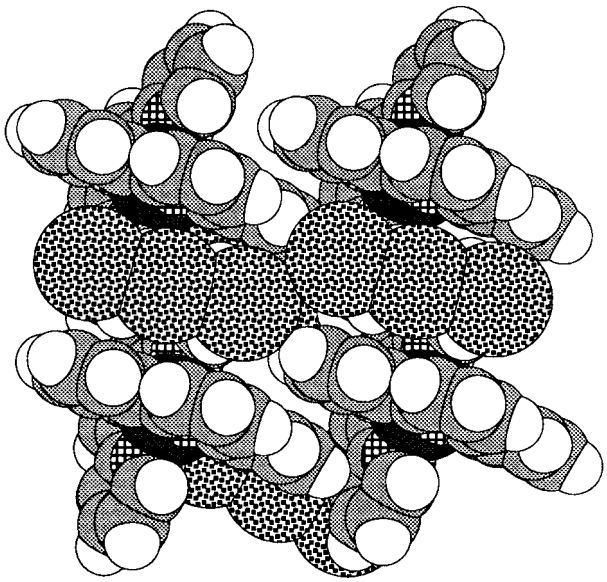

**Fig. 3** Space-filling representation of one side of the layer in $[Mn(terpy)_2](I_3)_2$ [SIWFIN], showing the $I_3^-$ ions lying in and along the grooves.

The two-dimensional terpy embrace motif allows some geometric variability, which is demonstrated in its various crystalline forms. Details of the crystallography of the motif are described in the supplementary information, but here we outline the primary characteristics and secondary variables of the motif in $[M(terpy)_2]^{2+}$ compounds. The layer of M atoms can be exactly planar, or can deviate by up to 1 Å from their mean plane. The terpy ligand planes (which are usually within 5° of orthogonality within the complex) are sometimes exactly orthogonal to the layer plane, but can tilt by up to 25°. The two sides of the terpy layer motif can be identical, or slightly different. Adjacent layers are always offset so that H4′ is positioned in the grooves of contiguous layers, and ligand planes in adjacent layers can be orthogonal or rotated by 45°. Crystal symmetry can be high (tetragonal space group $P4_2/n$) or low, and very often the unit cell dimensions are close to 9 Å × 9 Å × 20 Å, or a multiple of this (including 12.5 Å × 12.5 Å × 40 Å).

It is noteworthy that many of the crystals with this terpy layer motif contain solvent, and most of the structures in Table 1 exhibit disorder of the anion, or of solvent, or of both, but not of the $[M(terpy)_2]^{2+}$ cations. These properties are characteristic of lattices in which there is a dominant but relatively invariant supramolecular motif, and support this interpretation of the layers of terpy embraces.

There are two crystal structures (see Table 1) with tricationic $[M(terpy)_2]^{3+}$, both associated with monoanions, which therefore increases the number of anions and partially disrupts the terpy layer motif. In the case of $[Co(terpy)_2]^{3+}$ with $Cl^-$ and water [CAPRIU], the $[Co(terpy)_2]^{3+}$ ions pack within layers, but aryl···aryl interactions are restricted to one direction, forming chains of molecules. Interactions in the other direction in the layer are disrupted by the unusually large number (eleven) of water molecules present. $[Cr(terpy)_2]^{3+}$ with perchlorate [TERPCR] has a distorted layer structure where some of the aryl···aryl interactions are lost.

### Disruption of $[M(terpy)_2]^{2+}$ embraces

One measure of the significance of a supramolecular motif is the extent to which it resists disruption, by the geometrical packing requirements of associated species such as the counter ions, or by energetically more favourable alternative motifs. What does it take to disrupt the two-dimensional motif of

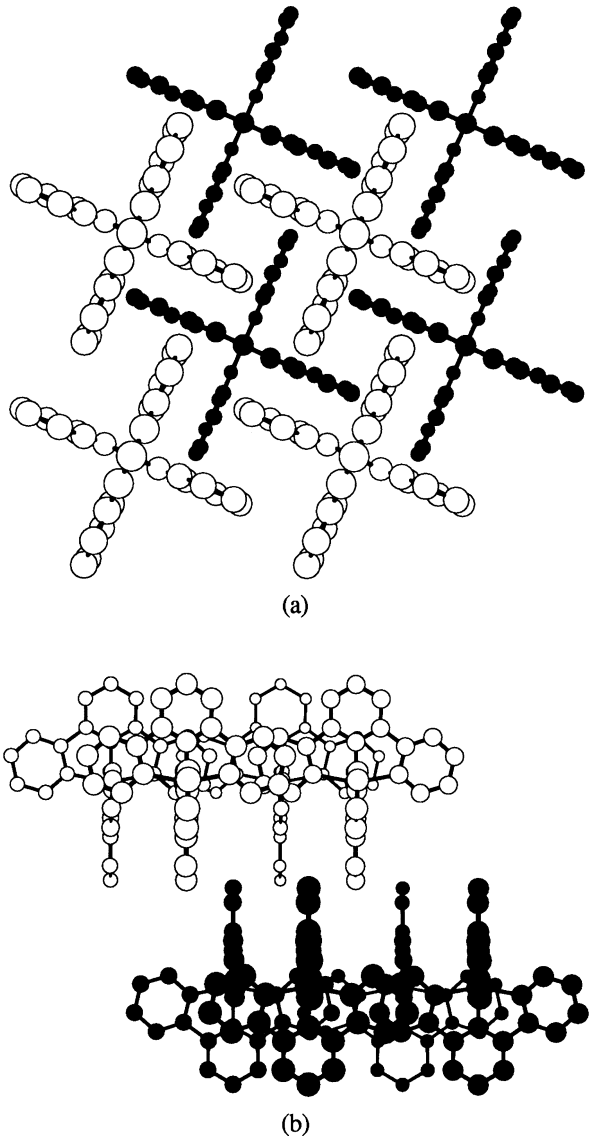


**Fig. 4** Relative locations and orientations of $[Co(terpy)_2]^{2+}$ molecules in two contiguous nets of terpy embraces in $[Co(terpy)_2]I_2 \cdot 2H_2O$ [CASXID]. (a) View perpendicular to the net: the upper layer is white, and H atoms are not drawn. The protruding C4′–H4′ bond on the $S_4$ axis of each molecule is directed midway between four molecules in the next layer. (b) Contiguous ligands across the layer interface are parallel.

terpy embraces? Clearly, it would be impossible for the layer to form with very large anions, unless the anions were able to form their own discrete layer. Crystallised with the anion $Ph_4B^-$, $[Co(terpy)_2]^{2+}$ forms crystals [NACPOW] from nitrobenzene in which each cation is surrounded by anions and solvent, so that there are cation···anion and cation···solvent aryl···aryl interactions and the presence of phenylated anion and solvent has completely disrupted the layer structure. On the other hand, the structure of $[Fe(terpy)_2]^{2+}$ crystallised with the complex anion $[Fe(dipicolinate)_2]^-$, in the presence of acetonitrile and water [ZIMBUS] retains cation···cation interactions in the form of linear chains of P4AE.

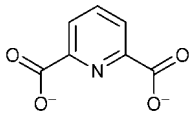


dipicolinate$^{2-}$

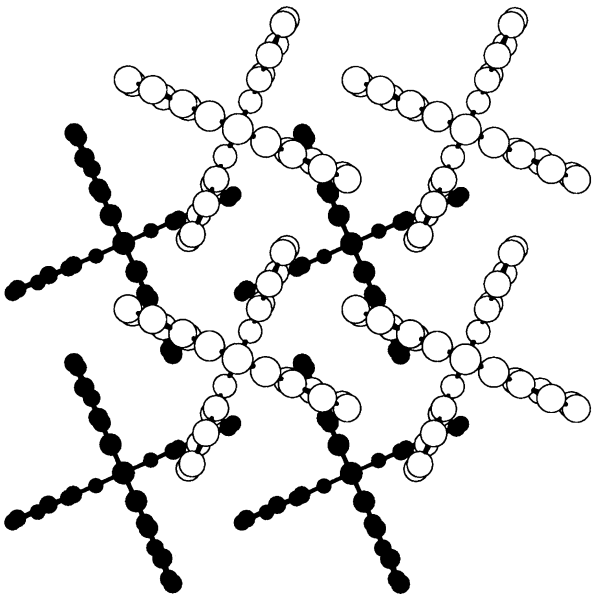

**Fig. 5** Projection perpendicular to the layers in $[Cu(terpy)_2](PF_6)_2$ [BEJPUB] showing the relative locations and orientations of molecules in adjacent layers.

The only other $[M(terpy)_2]^{2+}$ crystal structures that do not form the two-dimensional net of terpy embraces are $[Hg(terpy)_2](F_3CSO_3)_2 \cdot 0.5$(acetone) [ZUWPEM] and $[Mg(terpy)_2][Mg(terpy)(H_2O)_3]Br_4 \cdot$(2-propanol) [TAQRUY]. In ZUWPEM the layer structure is maintained but the ligand planes are substantially tilted from being orthogonal to the plane, and the ligands protruding from the layer are not all parallel. In TAQRUY the lattice contains $[Mg(terpy)_2]^{2+}$ taking part in P4AE, and $[Mg(terpy)(H_2O)_3]^{2+}$ with their terpy ligands in **off** arrangement.

Before reporting the calculated energies of the terpy embrace motif, we describe some crystal structures of other metal complexes that provide additional insight into this motif.

### The two-dimensional terpy embrace motif for $[M(L)_2]^{2+}$ with other ligands

Table 2 contains details of crystal structures of $ML_2$ compounds in which L is a meridional tridentate $N_3$ donor ligand, but without some of the pyridyl rings of terpy. There is a variety of crystal packing in these structures: some illustrate the two-dimensional net of aryl embraces very similar to the terpy embrace, some contain slightly modified planar arrays, and some have no planar array.

**Modification of one R°.** In $[Ru(terpy)(L^a)](BF_4)_2 \cdot 2CH_3CN$ [ZUMXUA] the ligand $L^a$ is a variant of terpyridine in which one outer pyridyl ring is *N*-methylated. Tridentate coordination by $L^a$ is achieved *via* a carbon atom of this ring, allowing the terpy embrace motif to be retained in the crystal.

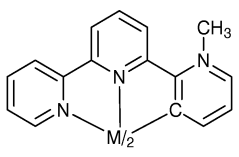


$L^a$

**Modification of both R°.** $[Fe(L^b)_2](ClO_4)_2 \cdot H_2O$ [DIXDIX] has both R° replaced by thiazole rings in which the N atoms are the donor atoms. It crystallises with a triclinic cell of dimensions similar to those of the triclinic examples with

**Table 1** Crystals containing $[M(terpy)_2]^{z+}$, $z = 2,3$

| REFCODE | Metal | Anions, solvent, other components[a] | Terpy layer motif | Space group | Cell dimensions/ Å and ° |
|---|---|---|---|---|---|
| CASXID01[b] | Co(II) | $(I^-)_2 \cdot (H_2O)_2$[a] | ✓ | $P4_2/n$ | 8.9 × 19.4 |
| BEJPUB | Cu(II) | $(PF_6^-)_2$ | ✓ | $P\bar{4}2_1c$ | 8.9 × 20.6 |
| BIKJUA | Ni(II) | $(PF_6^-)_2$ | ✓ | $P2_12_12_1$ | 8.9 × 9.0 × 45.4 |
| CAPSAN | Co(II) | $(ClO_4^-)_2$[a] $\cdot (H_2O)_{1.3}$[a] | ✓ | $I4_1/a$ | 12.5 × 40.4 |
| BIYJOI[c] | Co(II) | $(ClO_4^-)_2$[a] $\cdot (H_2O)_{0.5}$[a] | ✓ | $I4_1/a$ | 12.5 × 40.3 |
| FADJAW | Co(II) | $(NO_3^-)_2$[a] $\cdot (H_2O)_2$ | ✓ | $I4_1/a$ | 12.4 × 38.9 |
| KUDCER | Mg(II) | $(ClO_4^-)_2 \cdot (H_2O)_{0.5}$ | ✓ | $I4_1/a$ | 12.5 × 40.5 |
| TERPYC01 | Cu(II) | $(NO_3^-)_2$ | ✓ | $I4_1/a$ | 12.5 × 36.3 |
| Ref. 15 | Ru(II) | $(ClO_4^-)_2$[a] $\cdot (H_2O)_{1.1}$[a] | ✓ | $I4_1/a$ | 12.5 × 40.2 |
| DANMOU | Fe(II) | $(ClO_4^-)_2$[a] $\cdot H_2O$ | ✓ | $P2_1$ | 8.8 × 8.9 × 20.0 101 |
| ZARNIP | Ni(II) | $(ClO_4^-)_2$[a] $\cdot H_2O$ | ✓ | $P2_1$ | 8.8 × 8.9 × 20.1 99 |
| Ref. 15 | Os(II) | $(ClO_4^-)_2$[a] $\cdot (H_2O)_{0.5}$ | ✓ | $P2_1/n$ | 8.8 × 8.9 × 39.2 94 |
| SIBWEF | Cu(II) | $(Br^-)_2$[a] $\cdot (H_2O)_3$[a] | ✓ | $P\bar{1}$ | 20.0 × 9.7 × 8.5 96, 94, 95 |
| TPYCOB | Co(II) | $(Br^-)_2$[a] $\cdot (H_2O)_3$[a] | ✓ | $P\bar{1}$ | 19.8 × 9.6 × 8.5 96, 93, 94 |
| SIWFIN | Mn(II) | $(I_3^-)_2$ | ✓ | $P\bar{1}$ | 9.4 × 8.6 × 24.5 94, 96, 92 |
| TERPCO | Co(II) | $(SCN^-)_2$[a] $\cdot (H_2O)_2$[a] | ✓ | $P\bar{1}$ | 20.8 × 9.1 × 8.7 91, 91, 102 |
| TERPCO01 | Co(II) | $(SCN^-)_2 \cdot (H_2O)_2$ | ✓ | $P\bar{1}$ | 20.7 × 9.0 × 8.7 91, 91, 104 |
| ZUWPEM | Hg(II) | $(F_3CSO_3^-)_2$[a] $\cdot$ (acetone)$_{0.5}$ | ✓ modified | $P\bar{1}$ ($z = 2$) | 14.6 × 15.3 × 18.8 70, 71, 89 |
| NACPOW | Co(II) | $(BPh_4^-)_2 \cdot$ nitrobenzene | | $Pbcn$ | 20.7 × 17.0 × 19.3 |
| ZIMBUS | Fe(II) | $[(dipicolinato)_2Fe^-]_2 \cdot (CH_3CN)_3$[a] $\cdot H_2O$ | chains of P4AE | $P2_1/n$ | 8.9 × 37.4 × 19.0 100 |
| TAQRUY | Mg(II) | $[Mg(terpy)(H_2O)_3]^{2+} \cdot (Br^-)_4 \cdot Pr^iOH$ | P4AE | $P\bar{1}$ | 19.4 × 12.9 × 11.5 111, 99, 99 |
| CAPRIU | Co(III) | $(Cl^-)_3$[a] $\cdot (H_2O)_{11}$ | | $P\bar{1}$ | 9.0 × 11.8 × 18.1 91, 91, 91 |
| TERPCR | Cr(III) | $(ClO_4^-)_3 \cdot H_2O$ | | $Cc$ | 12.9 × 13.6 × 19.4 101 |

[a] Indicates some positional and/or orientational disorder. [b] CASXID is a low temperature study (120 K) with cell $a = b = 8.8$, $c = 19.3$ Å. [c] No coordinates available.

terpyridine. Despite the change in R°, the layer structure is maintained.

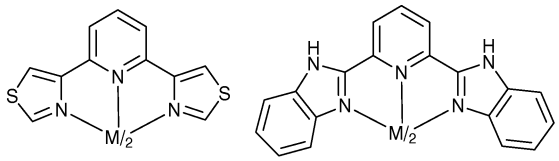


$L^b$ $L^c$

$[Fe(L^c)_2](F_3CSO_3)_2 \cdot 1.5EtOH$ [PAFZIF] has larger benzimidazole rings as R°, but still forms the layered structure of terpy embraces with 12 aryl···aryl interactions, as shown in Fig. 6. The grooves, which were previously occupied by the anions (and solvent), are now much shallower due to the terminal benzene rings, and the anions and solvent are therefore relegated to lie between the layers. In these crystals the ligand $L^c$ is also capable of taking part in hydrogen bonding *via* the imidazole NH groups, and hydrogen bonding of the type NH···O(EtOH)···O(triflate)···HN links molecules within the layer, but this does not disrupt the layer structure.

Another ligand with hydrogen bonding capability is $L^d$. In its complex, $[Fe(L^d)_2](F_3CSO_3)_2$ [RIZSOI], the layer structure persists, accompanied also by hydrogen bonding, NH···O(triflate). In a similar way, $[Ni(L^d)_2](BF_4)_2 \cdot 1.9H_2O$ [RIZSUO] maintains the layer of terpy embraces, but hydrogen bonding occurs on each of the two (different) sides of the layer, on one side with water and on the other side with $BF_4^-$ anion. The complex of the similar ligand, $L^e$, $[Fe(L^e)_2](BF_4)_2 \cdot 3H_2O$ [COLJAO], is very nearly isostructural with RIZSUO.

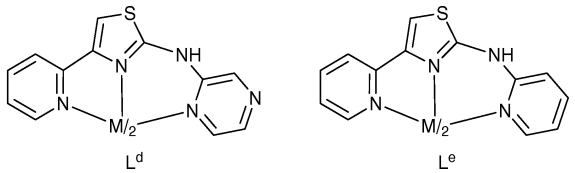


$L^d$ $L^e$

Evidently hydrogen bonding involving the ligand and/or the anion can coexist with the two-dimensional net of terpy embraces without disrupting it.

### Anion variation for $[Fe(L^f)_2]^{2+}$

There is an informative set of structures (see Table 2) in which different anions are crystallised with the iron(II) complex $[Fe(L^f)_2]^{2+}$ containing ligand $L^f$, which has two pyrazole rings as R°.[18]

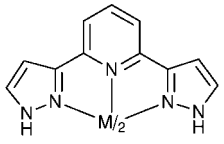


$L^f$

$L^f$ also is capable of hydrogen bonding *via* the NH groups. When the anion is $I^-$, as in $[Fe(L^f)_2]I_2 \cdot 4H_2O$ [WEYVUR],

**Table 2** Crystals containing $[M(L)_2]^{2+}$, where L is a terypyridine-like tridentate ligand

| REFCODE | Metal and ligands | Anions and solvent[a] | Space group | Cell dimensions/Å and ° |
|---|---|---|---|---|
| ZUMXUA | Ru(II)(terpy)($L^a$) | $(BF_4)_2 \cdot (CH_3CN)_2$ | $P4_1$ | 12.4 × 47.6 |
| DIXDIX | Fe(II)($L^b$)$_2$ | $(ClO_4)_2 \cdot H_2O$ | $P\bar{1}$ | 8.7 × 8.9 × 19.6<br>100, 101, 91 |
| PAFZIF | Fe(II)($L^c$)$_2$ | $(F_3CSO_3)_2 \cdot (EtOH)_2$ | $P\bar{1}$ | 10.6 × 13.6 × 17.8<br>74, 75, 76 |
| RIZSOI | Fe(II)($L^d$)$_2$ | $(F_3CSO_3)_2$ | $P\bar{1}$ | 8.8 × 11.1 × 17.5<br>78, 87, 84 |
| RIZSUO | Fe(II)($L^d$)$_2$<br>[one ligand discordered] | $(BF_4)_2{}^a \cdot (H_2O)_{1.9}{}^a$ | $P2_1/c$ | 8.8 × 8.8 × 41.2<br>95 |
| COLJAO | Fe(II)($L^e$)$_2$<br>[ligands disordered] | $(BF_4)_2{}^a \cdot (H_2O)_3{}^a$ | $P2_1/c$ | 9.0 × 9.0 × 41.2<br>95 |
| WEYVUR | Fe(II)($L^f$)$_2$ | $(I)_2 \cdot (H_2O)_4$ | $P\bar{1}$ | 8.3 × 8.3 × 21.9<br>98, 90, 91 |
| Ref. 16 | Fe(II)($L^f$)$_2$ | $(SeCN)_2$ | $P\bar{1}$ | 8.4 × 8.4 × 19.9<br>87, 83, 89 |
| Ref. 16 | Fe(II)($L^f$)$_2$ | $(SCN)_2 \cdot (H_2O)_4$ | $P\bar{1}$ | 8.3 × 8.4 × 21.5<br>79, 83, 90 |
| Ref. 17 | Fe(II)($L^f$)$_2$ | $(F_3CSO_3)_2 \cdot (H_2O)_3$ | $P\bar{1}$ | 11.5 × 12.2 × 13.7<br>105, 105, 104 |
| WEYWAY | Fe(II)($L^f$)$_2$ | $(BF_4)_2{}^a \cdot (H_2O)_3$ | $C2/c$ | 31.2 × 14.5 × 12.9<br>99 |
| KIJZUY<br>isostructural with<br>Zn, Fe, Cu | Mn(II)($L^g$)$_2$ | $H_2O$ | $P2_1/c$ | 9.2 × 8.8 × 28.9<br>97 |
| WEYWEC | Fe(II)($L^d$)$_2$<br>[deprotonated] | $(C_6H_6)_{1.5}$ | $P2_1/c$ | 14.9 × 12.6 × 16.8<br>95 |
| ACPXNI | Ni(IV)($L^h$)$_2$<br>[Ni on $\bar{4}$ site] | — | $I4_1/a$ | 7.7 × 30.5 |
| NAPYFE10 | Fe(II)($L^i$)$_4$ | $(ClO_4)_2$ | $P\bar{1}$ | 9.2 × 9.3 × 20.1<br>100, 77, 92 |

[a] Indicates some positional and/or orientational disorder.

the standard layer of terpy embraces is formed with the full complement of 12 aryl···aryl interactions. There are two different hydrogen-bonded arrays at terpy layer interfaces. Both involve hydrogen bonding between the >NH groups, $I^-$, and water. Both form chains of four-membered and six-membered hydrogen-bonded cycles, but on one side of the layers it is the $I^-$ that hydrogen bonds to the >NH group, while on the other it is water.

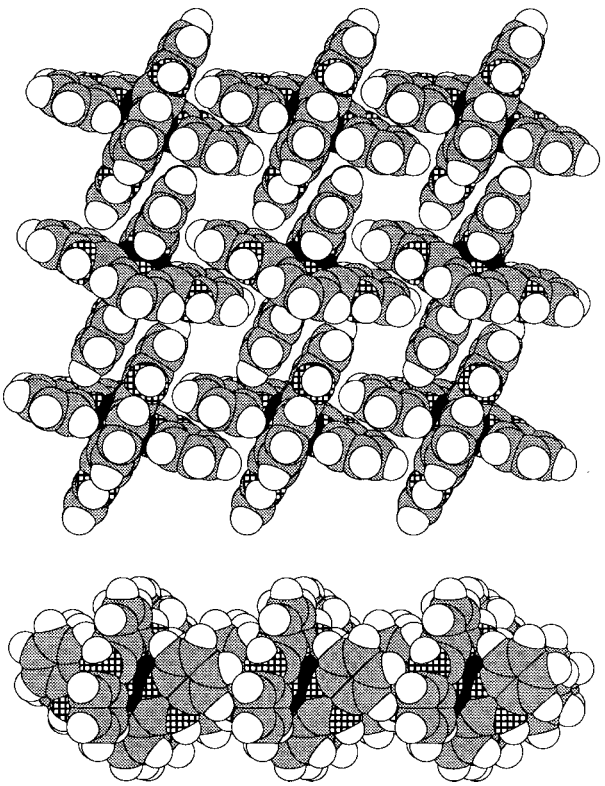

**Fig. 6** Perpendicular and parallel views of the layer motif formed by complexes $[Fe(L^c)_2]^{2+}$ in PAFZIF.

With the anion $SeCN^-$, $[Fe(L^f)_2]^{2+}$ crystallises anhydrously, while with $SCN^-$ it crystallises with water.[16] The layer of terpy embraces is formed in each instance accompanied by hydrogen bonding from the ligand (see Fig. 7). Crystallisation of $[Fe(L^f)_2]^{2+}$ with triflate yields a trihydrate from water, Table 2. The layer structure remains, but only nine of the twelve aryl···aryl interactions are retained, and the array of Fe atoms within the layer is distorted from rectangular towards hexagonal. There is a much larger cavity in the layer surface, which accommodates the triflate anion and water, as shown in Fig. 8. Crystallisation of $[Fe(L^f)_2]^{2+}$ with $BF_4^-$ from water [WEYWAY] yields a completely different lattice, with the disruption of virtually all aryl···aryl interactions, and almost complete isolation of the cations (see supplementary information).

## Neutral complexes $[ML_2]^0$

Terpy-like ligands capable of mono-deprotonation can form uncharged complexes $[ML_2]^0$. It is conceivable that such complexes could crystallise with the classic layered terpy embrace motif, and that—being free of anions—the adjacent layers could interpenetrate each other such that the protuberant rings of one layer fit into the grooves of the other. Only a few crystal structures of such complexes have been reported, some with included solvent and some without, as listed in Table 2. The two examples with solvent in the lattice are $[Mn(L^g)_2] \cdot H_2O$ [KIJZUY] and $[Fe(L^e - H)_2] \cdot 1.5C_6H_5$ [WEYWEC]. The first, KIJZUY, is made up of slightly distorted layers, but despite the distortion each molecule takes part in the 12 aryl···aryl interactions of the terpy embrace. In contrast, WEYWEC crystallises with only parts of the terpy embrace motif and incorporates chains of included benzene solvent taking part in **ef** interactions mainly with the aromatic rings of the cations.

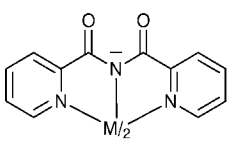

$L^g$

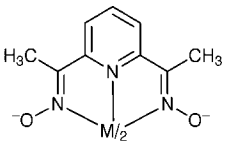

$L^h$

The expected interpenetrating terpy embrace layers do occur in the crystal structure of the Ni(IV) complex $[Ni(L^h)_2][ACPXNI]$,[19] and Fig. 9 shows how these layers fit together in the crystal lattice. The space group is $I4_1/a$, but unlike the isostructural group of compounds in that space group in Table 1, this structure has the metal atom occupying a $\bar{4}$ site. The ligand contains only the central ring $R^c$, which is engaged in local interlayer **off** interactions where this ring of one layer fits between equivalent rings of the contiguous layer. The absence of $R^o$ in $L^h$ means that the **ef** interactions that characterise the terpy embrace cannot form, but instead there are weak C–H···O hydrogen bonds (see Fig. 9).

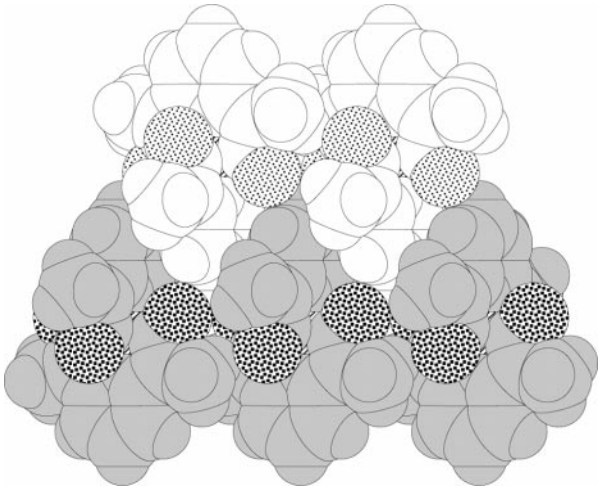

**Fig. 9** Side view of the terpy embrace layers in the crystal structure of $[Ni(L^h)_2][ACPXNI]$. Molecules in the two layers are differentiated by their light or dark shading. The deep mutual penetration of the layers is evident, as are the intermolecular interlayer C–H···O hydrogen bonds from methyl to oximate oxygen (stippled): H···O = 2.52 and C···O = 3.36 Å.

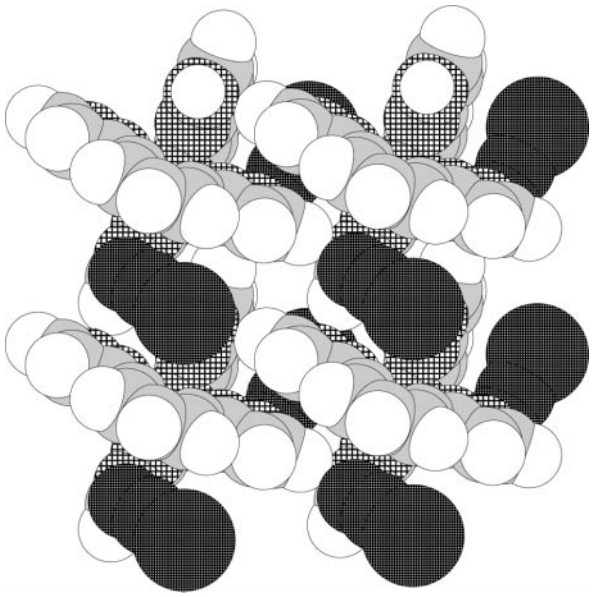

**Fig. 7** The terpy embraces in the crystal structure of $[Fe(L^f)_2](SeCN)_2$ showing the standard layer of interactions and the location of the anions. The anions have been emphasised by their dark shading (Se larger than C or N). The hydrogen bonding which accompanies the formation of this layer is perpendicular to the viewing plane and is to both N and Se of the anion.

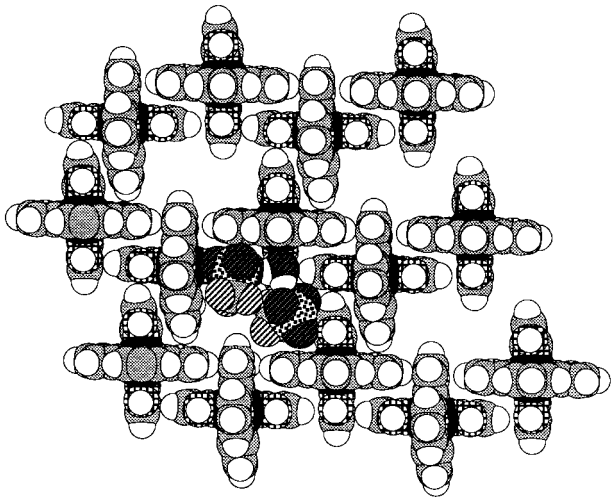

**Fig. 8** The distorted layer motif in the crystal structure of $[Fe(L^f)_2](F_3CSO_3)_2 \cdot 3H_2O$. The anions and solvent enclosed in one enlarged cavity of the layer are shown.

### A complex [M(bidentate)$_4$] forming the layered terpy motif

The edge-to-face and offset-face-to-face interactions that sustain the terpy embrace involve only the outer rings of the ligand. The possibility of a similar layer of concerted aryl embraces formed by a molecule in which the central ring $R^c$ is completely missing from the ligand is realised in an iron complex coordinated by four naphthyridine ligands $L^i$.

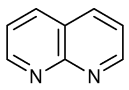

$L^i$

The ligands occur as two coplanar pairs, simulating the $R^o$ of terpy. The metal coordination stereochemistry, shown in Fig. 10, is compressed tetrahedral in terms of the centres of the N–N donor pairs. In the crystalline complex with perchlorate, $[Fe(L^i)_4](ClO_4)_2$ [NAPYFE10], the packing of the cations is essentially the same as that of the two-dimensional terpy embrace motif, with one very good **ef** interaction, while the **off** interaction is somewhat splayed from ideal [see Fig. 10(b)], as is the second **ef** interaction. The unit cell has the standard dimensions of 9 Å × 9 Å × 20 Å (see Table 2). The tridentate ligand has been replaced by two coplanar bidentate ligands in the layered terpy embrace motif.

### Energies of the terpy embrace motifs

The consistent occurrence of the two-dimensionally networked terpy embrace is testament to its favourability as a supramolecular motif, and must signify a major contribution to the overall lattice packing energies. Fundamental understanding of this supramolecular motif requires data on the magnitudes of the attractive energies. We have approached this through calculations of the intermolecular energies (using the summed atom–atom energy approximation) for the terpy embrace and for the cation–anion associations that occur in these crystals. Our intermolecular potential for atoms with charges $q_i$, $q_j$ separated by $d_{ij}$ is given in eqn. (1), with a distance-dependent permittivity.

$$E_{ij} = e^a_{ij}[(d^a_{ij}/d_{ij})^{12} - 2(d^a_{ij}/d_{ij})^6] + q_i \cdot q_j/\varepsilon \cdot d_{ij} \qquad (1)$$

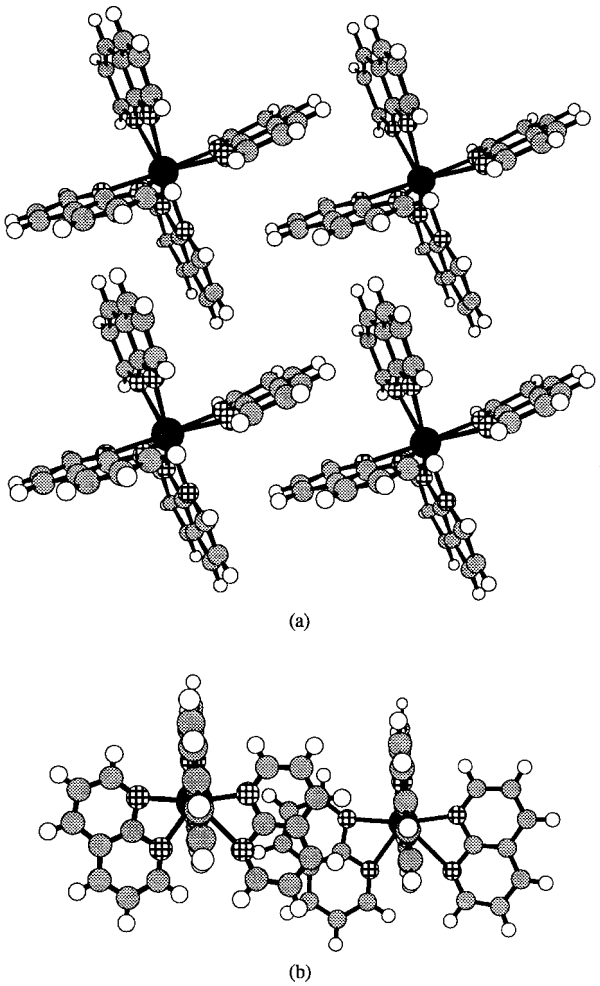

**Fig. 10** Representations of the crystal structure of the naphthyridine complex $[Fe(L^i)_4](ClO_4)_2$ [NAPYFE10], showing (*a*) part of the net of terpy embraces and (*b*) the **off** overlap of two naphthyridine ligands.

**Table 3** Atom parameters used in the calculation of supramolecular energies

| Van der Waals parameters | | |
|---|---|---|
| Atom | $e^a$/kJ mol$^{-1}$ | $r^a$/Å |
| C in terpy | 0.460 | 1.94 |
| H in terpy | 0.084 | 1.62 |
| N in terpy | 0.460 | 1.95 |
| M | 0.627 | 2.20 |
| I in $I^-$ | 2.84 | 2.6 |
| I in $I_3^-$ | 2.51 | 2.4 |
| Cl in $ClO_4^-$ | 1.00 | 2.0 |
| O in $ClO_4^-$ | 0.502 | 1.95 |
| P in $PF_6^-$ | 1.09 | 2.25 |
| F in $PF_6^-$ | 0.502 | 1.65 |
| H in $H_2O$ | 0.084 | 1.5 |
| O in $H_2O$ | 0.543 | 2.0 |

Calculated atom charges for $[M(terpy)_2]^{2+}$

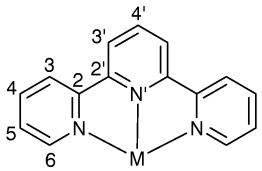


| Atom | $q$ | Atom | $q$ |
|---|---|---|---|
| M | +0.50 | | |
| N | −0.26 | | |
| N′ | −0.28 | | |
| C2 | +0.16 | | |
| C3 | −0.10 | H3 | +0.13 |
| C4 | −0.06 | H4 | +0.17 |
| C5 | −0.08 | H5 | +0.16 |
| C6 | +0.06 | H6 | +0.13 |
| C2′ | +0.13 | | |
| C3′ | −0.11 | H3′ | +0.13 |
| C4′ | −0.07 | H4′ | +0.18 |

Other atom charges: $I_3^- = I^{-0.39}$–$I^{-0.22}$–$I^{-0.39}$, $ClO_4^- = Cl^{+0.12}(O^{-0.28})_4$, $PF_6^- = P^{+0.80}(F^{-0.30})_6$

The coulombic component of the energy is significant, but its estimation is very dependent on the atomic partial charges and the permittivity. We have evaluated atom charges for inorganic molecules obtained by various methods including the QEq procedure of Rappe and Goddard[20] and the Mulliken, Hirshfeld and electrostatic potential (ESP) analyses of electron density obtained by density functional calculations. The atom parameters $e^a$, $d^a$ and $q$ are obtained by analyses described and justified in detail in a separate paper:[21] here we

**Table 4** Calculated intermolecular energies (kJ mol$^{-1}$) for embracing $[M(terpy)_2]^{2+}$ complexes and associated anions in crystals

| Structure | Local interaction | Total energy/ kJ mol$^{-1}$ | van der Waals energy/kJ mol$^{-1}$ | Coulombic energy/ kJ mol$^{-1}$ |
|---|---|---|---|---|
| CASXID $[Co(terpy)_2]^{2+}$ $2I^-$ | Complex 1···Complex 2 terpy embrace | −15 | −54 | 39 |
| | Complex 1···$I^-$ in groove | −44 | −4 | −40 |
| CAPSAN $[Co(terpy)_2]^{2+}$ $2ClO_4^-$ | Complex 1···Complex 2 terpy embrace | −15 | −54 | 39 |
| | Complex 1···$ClO_4^-$ in groove | −41 | −3 | −38 |
| | Complex 2···$ClO_4^-$ in groove | −46 | −5 | −41 |
| SIWFIN $[Mn(terpy)_2]^{2+}$ $2I_3^-$ | Complex 1···Complex 2 terpy embrace | −12 | −51 | 39 |
| | Complex 1···$I_3^-$ parallel to groove | −68 | −33 | −35 |
| | Complex 2···$I_3^-$ parallel to groove | −68 | −35 | −33 |
| | Complex 1···$I_3^-$ transverse to groove | −45 | −17 | −28 |
| | Complex 2···$I_3^-$ transverse to groove | −31 | −8 | −23 |
| BEJPUB $[Cu(terpy)_2]^{2+}$ $2PF_6^-$ | Complex 1···Complex 2 terpy embrace | −13 | −51 | 38 |
| | Complex 1···$PF_6^-$ within groove | −35 | −3 | −32 |
| | Complex 2···$PF_6^-$ within groove | −60 | −21 | −39 |
| | Complex 1···Complex 2 in contiguous layers | 14 | −9 | 23 |

comment that the van der Waals attractive energy $e^a$ for carbon in terpy has been increased slightly in accordance with the increased polarisability of these π-delocalised complexes, and the permittivity is set at $\varepsilon = 2d_{ij}$ for similar reasons. The parameters used for the calculations reported in this paper are contained in Table 3.

Calculated energies are reported for four representative terpy embrace motifs associated with different anions, in $[Co(terpy)_2]I_2 \cdot 2H_2O$ [CASXID], $[Co(terpy)_2](ClO_4)_2 \cdot 1.3H_2O$ [CAPSAN], $[Cu(terpy)_2](PF_6)_2$ [BEJPUB] and $[Mn(terpy)_2](I_3)_2$ [SIWFIN]. The results are collected in Table 4. These calculations show that the single terpy embrace between a pair of $[M(terpy)_2]^{2+}$ cations is but moderately attractive, with a net energy of *ca.* $-15$ kJ mol$^{-1}$. The distributed 2+ charge of the complex causes a small net repulsive electrostatic contribution to the intermolecular energy. Considering the two-dimensional net of terpy embraces, the attractive cation···cation energy per cation due to its four nearest neighbours is of the order of 30 kJ mol$^{-1}$. As would be expected there are large attractive energies between the cations and anions within the grooves of the layer, ranging from 35 to 68 kJ mol$^{-1}$. When these are added to the cation···cation energies, the result is very significant, *ca.* 130 kJ mol$^{-1}$ attraction per cation in the layer. Note that these are not the lattice energies, because only the nearest neighbours have been included. The data for BEJPUB in Table 4 show that there is net repulsion between $[Cu(terpy)_2]^{2+}$ complexes in contiguous layers, in contrast to the attractive terpy embrace within the layers resulting from the concert of **ef** and **off** interactions.

## Discussion

We have demonstrated the general occurrence of the terpy embrace between pairs of coordination complexes $[M(terpy)_2]^{2+}$, and complexes with a variety of related meridional tridentate ligands. Extension of this local embrace to the planar two-dimensional net is general, as long as the associated anions are not too large to interfere: each $[M(terpy)_2]^{2+}$ complex is engaged in eight **ef** and four **off** interactions. The intermolecular energy for a single terpy embrace is estimated to be *ca.* 15 kJ mol$^{-1}$ attraction per pair of $[M(terpy)_2]^{2+}$.

Associated anions and solvent are located in or near the grooves in the surfaces of the two-dimensional net of terpy embraces. Estimated energies for anion···cation pairs in these crystals range from 30 to 70 kJ mol$^{-1}$ attraction per pair. The anions clearly stabilise the layer of terpy embraces, but need not be engaged in specific interactions with the cations, and are generally observed to be crystallographically disordered. Solvent can be present in various amounts, and being often disordered appears to play a space-filling role in these crystals. The stability of the layer is demonstrated by the one structure where the $[M(tridentate)_2]$ complex is uncharged and crystallises without solvent $\{[Ni(L^h)_2]$ [ACPXNI]$\}$, allowing mutual interpenetration of the grooves in the layers of terpy-like embraces. Another $[M(tridentate)_2]^0$ complex, $[Mn(L^g)_2]$ [KIJZUY], crystallises with the terpy embrace layers slightly distorted by co-crystallised water. A different complex $[Fe(L^e - H)_2]^0$ [WEYWEC] crystallises with benzene, which disrupts the 12 aryl···aryl interactions of the terpy layer.

This layer structure is another crystal supramolecular motif based on concerted edge-to-face and offset-face-to-face aryl···aryl interactions. It provides considerable opportunity as a crystal supramolecular synthon involving metal sites with controllable electronic, magnetic and optical properties. The original recognition of the pattern of crystal packing in $[Co(terpy)_2]^{2+}$ complexes was concerned with subtleties in spin state and magnetism,[12] and many of the other $[Fe(N_3\text{-tridentate})_2]$ complexes that demonstrate the layer motif manifest spin state crossover.[22] It is interesting that in certain iron(II) spin crossover systems of the type $[Fe(bidentate)_2(NCS)_2]$ the observed cooperativity associated with the spin change has been ascribed to aryl···aryl interactions.[23,24] Although some $[Fe(L^f)_2]^{2+}$ salts also display cooperative spin crossover behaviour, the propagation of the spin change through the lattice by aryl···aryl interactions has not so far been established.

We have considered some of the issues for deployment of this two-dimensional supramolecular motif in crystal engineering. First we note that the layer motif is adopted by crystals of varying crystal symmetry, from triclinic to monoclinic to tetragonal. Even within a crystal system, there is space group variation, but the overall layer structure is maintained, and patterns are evident in the dimensions of the unit cells. The two compounds, $[M(terpy)_2]^{2+}$, M = Cu and Ni, both with the anion $PF_6^-$, crystallise in the different space groups $P\bar{4}2_1c$ and $P2_12_12_1$, respectively. The overall geometry of the two cations presents no clue as to why these compounds crystallise in different space groups, and so it is reasonable to conclude that the difference in lattice energy of the two crystal forms is not significant, and that under different crystallisation conditions, it should be possible to crystallise each in the other space group. Such polymorphism is quite likely for the other complexes listed in Table 1.

Associated anions can influence the crystal structure through their charge as well as size. There is still limited information on crystals where the ratio of anions to cations is not 2 : 1. Two examples of crystal structures of $[M(terpy)_2]^{3+}$, given in Table 1, both exhibit layer packing, but some of the 12 aryl···aryl interactions are lost. It is reasonable to propose that a similar disruption to the terpy layer structure would occur if a dianion were used with $[M(terpy)_2]^{2+}$, but we are not aware of any example of this in the literature. The energy of the terpy embrace is diminished as the oxidation state of the metal increases and disperses partial positive charge over the metal chelate, just as the sixfold aryl embraces between $[M(bipy)_3]^z$ complexes lose attractive energy as the charge $z$ increases from 2 to 3.[11]

Could the two-dimensional net of terpy embraces compete with hydrogen bonding in crystal engineering? We note that many of the crystals that contain the motif were crystallised from aqueous solution, and included small and variable amounts of water, almost always in the interlayer space. It is yet to be determined whether the terpy embrace can be sustained in the presence of more elaborate hydrogen bonding.

When the ligand is not terpy, but a related $N_3$ heterocyclic ligand that forms $ML_2$ with meridional stereochemistry, the terpy embrace layer structure is often maintained. The terpy embrace can occur when the central ring $R^c$ of the tridentate ligand is missing and, with modified local interactions, if the outer rings $R^o$ are missing. If the heterocyclic rings incorporate functional groups capable of hydrogen bonding, then there is the prospect of interference by hydrogen bonding in place of the aryl···aryl interactions that are the basis of the terpy embrace. We have found examples where the two types of intermolecular interaction in fact coexist with little modification of the layer structure. However, in some instances the hydrogen bonding is dominant, to the extent that the layer is not formed at all.

### Relationship to supermolecular grids

Being comprised of a square grid of octahedral metal complexes, this two-dimensional terpy embrace supramolecular motif is analogous to the supermolecular grids of metal centres synthesised by Lehn *et al.*[25–28] The differences are that the crystal supramolecular grid is two-dimensionally infinite and maintained by intermolecular energies, while Lehn's

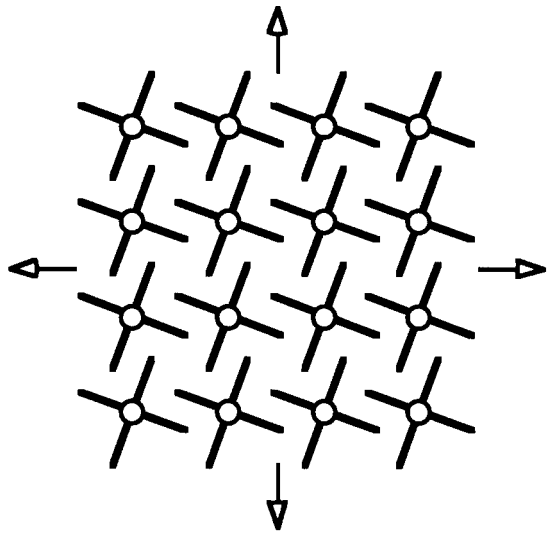

(a)

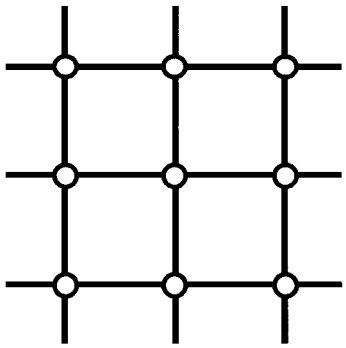

(b)

**Fig. 11** Diagrammatic comparison of the two-dimensional supramolecular net of terpy embraces (a) and the supermolecular grids (b) of Lehn: the circles are metal centres.

supermolecules are maintained by covalent bonds, and are finite. The similarities and differences are illustrated in Fig. 11.

We are investigating further the characteristics, consequences, and deployment of the two-dimensional net of terpy embraces.

## Acknowledgements

The support of this research by the Australian Research Council is gratefully acknowledged.

## References

1 I. G. Dance, in *The Crystal as a Supramolecular Entity*, ed. G. R. Desiraju, John Wiley, New York, 1996, pp. 137–233
2 I. G. Dance and M. L. Scudder, *J. Chem. Soc., Dalton Trans.*, 1996, 3755.
3 I. G. Dance and M. L. Scudder, *Chem. Eur. J.*, 1996, **2**, 481.
4 I. Dance and M. Scudder, *J. Chem. Soc., Chem. Commun.*, 1995, 1039.
5 I. Dance and M. Scudder, *New J. Chem.*, 1998, **22**, 481.
6 M. Scudder and I. Dance, *J. Chem. Soc., Dalton Trans.*, 1998, 329.
7 I. Dance and M. Scudder, *Polyhedron*, 1997, **16**, 3545.
8 C. Hasselgren, P. A. W. Dean, M. L. Scudder, D. C. Craig and I. G. Dance, *J. Chem. Soc., Dalton Trans.*, 1997, 2019.
9 M. Scudder and I. Dance, *J. Chem. Soc., Dalton Trans.*, 1998, 3167.
10 M. Scudder and I. Dance, *J. Chem. Soc., Dalton Trans.*, 1998, 3155.
11 I. Dance and M. Scudder, *J. Chem. Soc., Dalton Trans.*, 1998, 1341.
12 B. N. Figgis, E. S. Kucharski and A. H. White, *Aust. J. Chem.*, 1983, **36**, 1537.
13 F. H. Allen, J. E. Davies, J. J. Galloy, O. Johnson, O. Kennard, C. F. Macrae and D. G. Watson, *Chem. Inf. Comput. Sci.*, 1991, **31**, 204.
14 F. H. Allen and O. Kennard, *Chem. Des. Automat. News*, 1993, **8**, 131.
15 D. C. Craig, M. L. Scudder, W.-A. McHale and H. A. Goodwin, *Aust. J. Chem.*, 1998, **51**, 1131.
16 K. H. Sugiyarto, D. C. Craig, M. L. Scudder and H. A. Goodwin, unpublished results.
17 K. H. Sugiyarto, K. Weitzner, D. C. Craig and H. A. Goodwin, *Aust. J. Chem.*, 1997, **50**, 869.
18 K. H. Sugiyarto, D. C. Craig, A. D. Rae and H. A. Goodwin, *Aust. J. Chem.*, 1994, **47**, 869.
19 G. Sproul and G. D. Stucky, *Inorg. Chem.*, 1973, **12**, 2898.
20 A. K. Rappe and W. A. Goddard, *J. Phys. Chem.*, 1991, **95**, 3358.
21 B. F. Ali, I. G. Dance and M. L. Scudder, 1999, in preparation.
22 P. Gutlich, J. Jung and H. A. Goodwin, in *Molecular Magnetism: From Molecular Assemblies to the Devices*, eds. E. Coronado, P. Delhaes, D. Gatteschi and J. S. Miller, Kluwer Academic Publishers, Dordecht, The Netherlands, 1996, pp. 327–378.
23 Z. J. Zhong, J.-Q. Tao, Z. Yu, C.-Y. Dun, Y.-J. Liu and X.-Z. You, *J. Chem. Soc., Dalton Trans.*, 1998, 327.
24 J.-F. Letard, P. Guionneau, L. Rabardel, J. A. K. Howard, A. E. Goeta, D. Chasseau and O. Kahn, *Inorg. Chem.*, 1998, **37**, 4432.
25 P. N. W. Baxter, J. M. Lehn, J. Fischer and M. T. Youinou, *Angew. Chem., Int. Ed. Engl.*, 1994, **33**, 2284.
26 P. N. W. Baxter, J. M. Lehn, B. O. Kneisel and D. Fenske, *Chem. Commun.*, 1997, 2231.
27 D. M. Bassani, J. M. Lehn, K. Fromm and D. Fenske, *Angew. Chem., Int. Ed. Engl.*, 1998, **37**, 2364.
28 G. S. Hanan, D. Volkmer, U. S. Schubert, J. M. Lehn, G. Baum and D. Fenske, *Angew. Chem., Int. Ed. Engl.*, 1997, **36**, 1842.

## Refcode references

ACPXNI – G. Sproul and G. D. Stucky, *Inorg. Chem.*, 1973, **12**, 2898.
BEJPUB – M. I. Arriortua, T. Rojo, J. M. Amigo, G. Germain and J. P. Declercq, *Acta Crystallogr., Sect. B*, 1982, **38**, 1323.
BIKJUA – M. I. Arriortua, T. Rojo, J. M. Amigo, G. Germain and J. P. Declercq, *Bull. Soc. Chim. Belg.*, 1982, **91**, 337.
BIYJOI – W. Henke and S. Kremer, *Inorg. Chim. Acta*, 1982, **65**, L115.
CAPRIU – B. N. Figgis, E. S. Kucharski and A. H. White, *Aust. J. Chem.*, 1983, **36**, 1563.
CAPSAN – B. N. Figgis, E. S. Kucharski and A. H. White, *Aust. J. Chem.*, 1983, **36**, 1537.
CASXID, CASXID01 – B. N. Figgis, E. S. Kucharski and A. H. White, *Aust. J. Chem.*, 1983, **36**, 1527.
COLJAO – A. T. Baker, H. A. Goodwin and A. D. Rae, *Aust. J. Chem.*, 1984, **37**, 443.
DANMOU – A. T. Baker and H. A. Goodwin, *Aust. J. Chem.*, 1985, **38**, 207.
DIXDIX – A. T. Baker and H. A. Goodwin, *Aust. J. Chem.*, 1986, **39**, 209.
FADJAW – F. Takusagawa, P. G. Yohannes and K. B. Mertes, *Inorg. Chim. Acta*, 1986, **114**, 165.
KIJZUY – D. Marcos, J. V. Folgado, D. Beltran-Porter, M. T. P. Gambardella, S. H. Pulcinelli and R. H. De Almeida-Santos, *Polyhedron*, 1990, **9**, 2699.
KUDCER – E. C. Constable, J. Healy and M. G. B. Drew, *Polyhedron*, 1991, **10**, 1883.
NACPOW – A. L. Rheingold and M. B. Allen, private communication, 1996.
NAPYFE10 – P. Singh, A. Clearfield and I. Bernal, *J. Coord. Chem.*, 1971, **1**, 29.
PAFZIF – S. Ruttimann, C. M. Moreau, A. F. Williams, G. Bernardinelli and A. W. Addison, *Polyhedron*, 1992, **11**, 635.
RIZSOI, RIZSUO – B. J. Childs, J. M. Cadogan, D. C. Craig, M. L. Scudder and H. A. Goodwin, *Aust. J. Chem.*, 1997, **50**, 129.
SIBWEF – J. V. Folgado, W. Henke, R. Allmann, H. Stratemeier, D. Beltran-Porter, T. Rojo and D. Reinen, *Inorg. Chem.*, 1990, **29**, 2035.
SIWFIN – R. Bhula and D. C. Weatherburn, *Aust. J. Chem.*, 1991, **44**, 303.
TAQRUY – A. F. Waters and A. H. White, *Aust. J. Chem.*, 1996, **49**, 147.
TERPCO, TERPCO01 – C. L. Raston and A. H. White, *J. Chem. Soc., Dalton Trans.*, 1976, 7.
TERPCR – W. A. Wickramasinghe, P. H. Bird, M. A. Jamieson and N. Serpone, *J. Chem. Soc., Chem. Commun.*, 1979, 798.

TERPYC01 – R. Allmann, W. Henke and D. Reinen, *Inorg. Chem.*, 1978, **17**, 378.
TPYCOB – E. N. Maslen, C. L. Raston and A. H. White, *J. Chem. Soc., Dalton Trans.*, 1974, 1803.
WEYVUR, WEYWAY – K. H. Sugiyarto, D. C. Craig, A. D. Rae and H. A. Goodwin, *Aust. J. Chem.*, 1994, **47**, 869.
WEYWEC – B. J. Childs, D. C. Craig, K. A. Ross, M. L. Scudder and H. A. Goodwin, *Aust. J. Chem.*, 1994, **47**, 891.
ZARNIP – A. T. Baker, D. C. Craig and A. D. Rae, *Aust. J. Chem.*, 1995, **48**, 1373.
ZIMBUS – P. Laine, A. Gourdon and J.-P. Launay, *Inorg. Chem.*, 1995, **34**, 5156.
ZUMXUA – D. A. Bardwell, A. M. W. C. Thompson, J. C. Jeffery, J. A. McCleverty and M. D. Ward, *J. Chem. Soc., Dalton Trans.*, 1996, 873.
ZUWPEM – D. Matkovic-Calogovic, Z. Popovic and B. Korpar-Colig, *J. Chem. Crystallogr.*, 1995, **25**, 453.

*Paper 9/00564A*